

***In silico* repurposing of drugs for pan-HDAC and pan-SIRT inhibitors: Consensus structure-based virtual screening and pharmacophore modeling investigations**

Pan-HDAC ve pan-SIRT inhibitörleri için *in silico* ilaç yeniden konumlandırma: Konsensüs yapı-temelli sanal tarama ve farmakofor modelleme arařtırmaları

Suat Sari ^a, Ahmet Avcı ^a, Ebru Koçak Aslan ^{a*}

^a Hacettepe University, Faculty of Pharmacy, Department of Pharmaceutical Chemistry, 06100, Ankara, Turkey

* Correspondence: Ebru Koçak Aslan

Hacettepe University Faculty of Pharmacy

Department of Pharmaceutical Chemistry

06100 Sıhhiye Ankara/TURKEY

Tel.: + 90 312 305 18 72

Fax: + 90 312 305 32 72

<https://orcid.org/0000-0003-0191-0746>

e-mail: ebrukocak@hacettepe.edu.tr

08.09.2020

15.03.2021

ABSTRACT

INTRODUCTION: Drug repurposing is a highly popular approach to find new indications for drugs, which greatly reduces time and costs for drug design and discovery. Non-selective inhibitors of histone deacetylase (HDAC) isoforms including sirtuins (SIRT) were showed to be effective in conditions like cancer. In this study, we identified a number of drugs molecules with potential to show pan-HDAC and pan-SIRT inhibitor activity by consensus structure-based virtual screening of FDA-approved drugs library using molecular docking to suggest drugs to be repurposed for HDAC-related indications.

METHODS: The FDA-approved drugs library was optimized using MacroModel. The crystal structures of HDAC1-4, 6-8, SIRT1-3, 5, 6 were prepared and the library was docked to each structure using Glide, FRED, and AutoDock Vina/PyRx. Consensus scores were derived from the docking scores obtained from each software. Pharmacophore modeling was performed using Phase.

RESULTS: According to the consensus scores, belinostat, bexarotene, and cianidanol emerged as top virtual pan-HDAC inhibitors; while alosetron, cinacalcet, and indacaterol as virtual pan-SIRT inhibitors. Pharmacophore hypotheses for these virtual inhibitors were also suggested through pharmacophore modelling, which were in agreement with the molecular docking models.

DISCUSSION AND CONCLUSION: The consensus approach enabled selection of the best performing molecules according to different software, as well as those with good scores against as many isoforms as possible, i.e., virtual pan-HDAC and pan-SIRT inhibitors. The study not only proposes potential drugs to be repurposed for HDAC and sirtuin-related diseases but also provides insights for designing potent de novo derivatives.

Keywords: drug repurposing, HDAC, sirtuin, consensus scoring, virtual screening, pharmacophore modeling

ÖZ

GİRİŞ ve AMAÇ: İlaç yeniden konumlandırma, ilaçlara yeni endikasyonlar bulmak için oldukça popüler bir yaklaşımdır ve bu, ilaç tasarımı ve keşfi için zaman ve maliyeti önemli ölçüde azaltır. Sirtüinleri (SIRT'ları) de içeren histon deasetilaz (HDAC) izoformlarının seçici olmayan inhibitörlerinin kanser gibi hastalıklarda etkili oldukları gösterilmiştir. Bu çalışmada, moleküler modelleme yardımıyla FDA onaylı ilaç kütüphanesinin yapı temelli konsensüs sanal tarama çalışmaları ile HDAC ile ilişkili hastalıklar için önerilmek üzere pan-HDAC ve pan-SIRT inhibitör aktivite gösterme potansiyeli olan bazı ilaç molekülleri belirlenmiştir.

YÖNTEM ve GEREÇLER: FDA onaylı ilaçlar kütüphanesi MacroModel ile optimize edilmiştir. HDAC1-4, 6-8, SIRT1-3, 5, 6 yapıları hazırkanarak kütüphane her bir protein yapısına Glide, FRED ve AutoDock Vina/PyRx ile kenetlenmiştir. Konsensüs skorları her programdan elde edilen kenetleme skorlarından türetilmiştir. Farmakofor modelleme Phase yardımıyla gerçekleştirilmiştir.

BULGULAR: Konsensüs skorlarına göre belinostat, beksaroten ve siyanidanol en iyi sanal pan-HDAC inhibitörleri, alosetron, sinakalset ve indakaterol ise en iyi sanal pan-SIRT inhibitörleri olarak öne çıkmıştır. Bu moleküllerden yola çıkılarak oluşturulan farmakofor hipotezleri de moleküler kenetleme modelleri ile uyumluluk göstermiştir.

TARTIŞMA ve SONUÇ: Konsensüs yaklaşımı, farklı yazılımlara göre en iyi performans gösteren moleküllerin yanı sıra, olabildiğince çok izoforma karşı (sanal pan-HDAC ve pan-SIRT inhibitörlerine) iyi skorlara sahip moleküllerin seçimine olanak sağlamıştır. Bu çalışma, HDAC ve sirtüin ile ilişkili hastalıklar için potansiyel ilaçların yeniden konumlandırılmasını içermekle birlikte güçlü de novo türevleri tasarlamak için de yol gösterici olmuştur.

Anahtar Kelimeler: ilaç yeniden konumlandırma, HDAC, sirtüin, konsensüs skora, sanal tarama, farmakofor modelleme

Introduction

Histone deacetylases (HDACs) are an enzyme class that cleave acetyl groups from ϵ -N-acetylated lysine residues of histone proteins, which wrap DNA molecules. HDAC activity causes DNA molecules to be wrapped more tightly leading to various epigenetic regulations [1]. Thus, great efforts were made in the past couple of decades to inhibit HDAC activity as a strategy to design compounds against a wide range of conditions such as neurodegenerative diseases, inflammatory diseases, cancer, diabetes, cardiovascular diseases, HIV infections etc. [1-4].

To date, 18 HDAC isoforms have been identified, which are classified into four classes (class I-IV) according to their sequence homology and tissue distribution (Table 1). Class I, II, and IV are zinc-dependent classical HDACs, i.e. they require a Zn^{2+} ion in their catalytic site for activity, whereas class III, also known as sirtuins (SIRTs), are a structurally distinct class, which depend on NAD^+ for catalytic activity [1]. Currently, crystallographic structure of human

HDAC1-4, 6-8, SIRT1-3, 5, and 6 are available, leading to an increase in high-throughput virtual screening (hVS) for design and identification of novel specific HDAC inhibitors [5,6], as well as drug repurposing efforts [7], which became a new approach in drug design as a means to reduce costs and attrition rates in clinical studies and speed up drug development process [8].

Although isoform-selective HDAC inhibition is required in many HDAC-related treatment strategies [9], pan-HDAC (e.g.: trichostatin A, vorinostat, and valproic acid) and pan-SIRT inhibitors (e.g.: nicotinamide) gained attraction for their clinical effectiveness in certain diseases, especially cancer (Fig. 1) [10-12]. Because most HDAC isoforms are associated with tumorigenesis and tumor progression, such polypharmacological approaches may prove more effective than isoform-specific inhibitors [13].

Molecular docking is an *in silico* method to predict preferred binding orientation and affinity of a ligand with respect to a receptor. Molecular docking has been used as a robust tool to identify hit matter as part of virtual screening for a long time. To improve virtual screening performance, consensus scoring is applied by combining scoring functions of multiple programs, which usually is considered more accurate than single-score methods [6].

In this study, we identified a number of drug molecules with potential to show pan-HDAC and pan-SIRT inhibitor activities using consensus structure-based (hVS) of the FDA-approved drugs library in order to suggest drugs to be repurposed accordingly. The study also suggests pharmacophore hypotheses for virtual pan-HDAC and pan-SIRT drugs through pharmacophore modelling, which are expected to improve our understanding to design potent *de novo* derivatives.

Methods

Ligand preparation

The FDA-approved drugs collection was obtained as 3D-coordinates sdf file from DrugBank (<http://www.drugbank.ca>) (accession: July 3, 2019) [14]. After removing the experimental, investigational, and nutraceutical compounds, the remaining 1502 ligands were prepared to remove salts and counter ions using LigPreP (2019-2, Schrödinger, LLC, New York, NY) and optimized geometrically using MacroModel (2019-2, Schrödinger, LLC, New York, NY) and conjugate gradients method according to OPLS_2005 forcefield parameters [15]. The optimized library was directly used for Glide (2019-2, Schrödinger, LLC, New York, NY) [16-18] and converted to sdf format for FRED (v3.3.1.2, Open Eye Scientific Software; Santa Fe, NM) [19]. For AutoDock Vina (v1.1.2, The Scripps Research Institute, San Diego, CA) the library was converted to pdbqt format by Open Babel (v2.4) [20].

Molecular docking protocol

The crystal structures of HDAC1-4, 6-8, SIRT1-3, 5, 6 were downloaded from the RCSB Protein Data Bank (www.rcsb.org) [21]. The protein structures were prepared for docking by removing unwanted chains and residues, adding missing atoms, assigning hydrogen atoms, bond orders, partial charges (for Glide only), and setting ionization and tautomeric states, as well as the H bonds of the protein residues using the Protein Preparation Wizard of Maestro (Epik, Impact, Prime: 2019-2, Schrödinger, LLC, New York, NY) [22]. The prepared protein structures were assigned Gasteiger charges and converted to their pdbqt format using AutoDockTools (v1.5.7, The Scripps Research Institute, San Diego, CA) for AutoDock Vina. Grid maps of the active site of each protein was prepared using the receptor grid generation panel of Maestro (2019-2, Schrödinger, LLC, New York, NY) for Glide, Make Receptor (v3.3.1.2, Open Eye Scientific Software; Santa Fe, NM) for FRED. This procedure is automatically performed by AutoDock Vina. The central coordinates of the catalytic site of each structure were taken for a grid box of

27x10³ Å³ size (see Electronic Supplementary Material for details). Molecular docking on Glide was performed at standard precision at 50 runs per ligand with the following settings: a scaling factor of 0.80 with charge cutoff 0.15 (absolute value) was applied for the ligands, Epik (2019-2, Schrödinger, LLC, New York, NY) state penalties were added to docking scores, nitrogen inversions and ring conformations were sampled, and post docking minimization was enabled. For FRED docking was performed at high resolution mode with 50 runs per ligand. For AutoDock Vina the default parameters were used and the virtual screening tool PyRx (v0.8, The Scripps Research Institute, San Diego, CA) was used run the docking simulations on AutoDock Vina [23]. Each ligand was assigned a docking score of the identified best pose from each software upon visual evaluation. Consensus score of a ligand for a given structure was determined by calculating the average of the three scores from the three software. A pan-HDAC and pan-SIRT score were determined for each ligand by calculating the average of the consensus scores for all HDAC and SIRT structures, respectively.

Pharmacophore modeling

3D pharmacophore models for pan-HDAC and pan-SIRT inhibitor drugs were created with Phase (2019-2, Schrödinger, LLC, New York, NY) [24] using the top-scoring three ligands according to each pan-HDAC (belinostat, bexarotene, and cianidanol) and pan-SIRT scores (alosetron, cinacalcet, and indacaterol) according to the following settings: Finding best alignment and common features method was applied, 50 conformers were generated for each ligand, three to five features were required in each hypothesis, all the query compounds were required to match each hypothesis, and the hypotheses (6 for pan-HDAC and 20 for pan-SIRT) were ranked according to PhaseHypoScore and the best hypothesis was selected for each group. The FDA-approved drug library was screened against each selected hypothesis using Phase Ligand Screening panel with the default settings.

Results and discussion

Consensus structure-based VS

1502 FDA-approved drug molecules were *in silico* screened against HDAC1-4, HDAC6-8, SIRT1-3, 5, and 6 using three different docking software. For each drug molecule, a consensus score was assigned regarding each HDAC and SIRT isoform, which was the mean of the scores from the three software. A pan-HDAC score was then determined for each molecule by calculating the mean of the consensus scores for HDAC1-4 and HDAC6-8 (Table 2). The pan-SIRT scores were calculated the same way using the consensus scores for SIRT1-3, 5, and 6 of each drug molecule (Table 3). By doing so, it was assured that the molecules not only with good scores from all of the software but also with good consensus scores for all the isoforms ranked higher.

Virtual pan-HDAC drugs

Among the classical HDAC isoforms, class I and II HDACs share a similar catalytic site topology. A zinc cofactor, chelating with two aspartate and one histidine residues, and a substrate, is at the bottom of a narrow lipophilic gorge that forms the catalytic site (Fig. 2). Therefore, compounds with a linear lipophilic moiety with H bond donor and acceptor groups at the tip such as trichostatin A can effectively occupy this site by chelating with the zinc and interacting with the zinc ligands. The active site of classical HDACs leaves little room for conformational flexibility, thus FRED, Glide, and AutoDock Vina usually produced similar poses for the molecules. Belinostat, bexarotene, and cianidanol were found top pan-HDAC scoring molecules in our study (Fig. 3).

Not surprisingly, as a pan-HDAC inhibitor anticancer drug, belinostat obtained the best pan-HDAC score. Belinostat ranked 6th according to consensus HDAC1 scores and 1st according to consensus HDAC2, 6, and 8 (see Electronic Supplementary Material for details). Indeed, belinostat's IC₅₀ values against these targets were reported as 7.20, 7.31, 7.82, and 7.16 nM [25-28]. A hydroxamic acid at the end of a cinnamyl moiety is typical of potent classical HDAC inhibitors. The hydroxamic acid moiety of belinostat was in close contact with the zinc and its ligands (Fig. 4a-c). The cinnamyl benzene stacked with the histidine ligand (e.g.: His709 of HDAC7) of zinc, as well as other aromatic sidechain of the nearby residues, e.g.: Phe679 and Phe738 of HDAC7, in HDAC active sites, which was in accordance with the previous findings [29] (see Electronic Supplementary Material for details).

Bexarotene, the second best pan-HDAC scoring drug, is also an antineoplastic drug approved for the treatment of cutaneous T cell lymphoma [30]. The retinoid X receptor activator has not been tested against any HDACs so far, but it obtained the 7th best consensus HDAC2 and the 2nd best consensus HDAC6 score in our study. The benzoic acid moiety of bexarotene was mainly responsible for binding to HDAC active sites, in which the carboxylate group interacted with the zinc, its ligands, and nearby residues like Tyr308 of HDAC2, and the benzene stacked with the aromatic side chains of the nearby residues such as Phe155 and Phe210 of HDAC2 (Fig. 4d-f). Bexarotene was also the 8th best pan-SIRT scoring molecule, making it a likely inhibitor of the HDACs of all classes.

Cianidanol ((+)-catechin) is a natural flavonol and a drug withdrawn due to hematological toxicity, however it is still marketed as an over-the-counter product for weight loss [31]. It has been clinically evaluated for several cancer types, but has no anti-HDAC activity record. In our study, it was the 2nd, 9th, and 4th best compound according to consensus HDAC4, 7, and 8 scores. Cianidanol is structurally different from the classical HDAC inhibitors regarding the zinc-interacting group, which is *ortho* phenolic hydroxyls instead of a hydroxamic or carboxylic acid. While these hydroxyl groups engaged with the zinc and its ligands, the benzene bearing the hydroxyls stacked with the aromatic side chains of the nearby residues such as Phe155 and Phe210 of HDAC2 like belinostat and bexarotene (Fig. 4g-i).

Virtual pan-SIRT drugs

Unlike HDACs, NAD⁺-dependent SIRT active site is more deeply buried and roomier, which is composed of NAD⁺-binding Rossmann-fold subdomain and a distal zinc-binding pocket (Fig. 2) [32]. The active pockets of SIRTs show large variations among the isoforms, thus binding modes among the drug molecules and among the software for the same molecule varied to certain extent with exceptions. Since apo (NAD⁺ free) and holo (NAD⁺ including) states of SIRTs are known to be inhibited by inhibitors of diverse topology [32,33], we preferred the apo form of SIRTs in hVS process not to miss out bulky drug molecules. Alosetron, cinacalcet, and indacaterol emerged as the best three drug molecules from the hVS study according to pan-SIRT scores (Fig. 3).

Alosetron is a "setron", i.e. 5-HT₃ receptor antagonist, used for the treatment of irritable bowel syndrome [34]. The effects of alosetron on SIRTs have yet to be studied, however it obtained the best pan-SIRT score and the 7th best consensus SIRT2 score. Alosetron appeared to have two important moieties for interacting with the relevant key SIRT residues: the imidazole ring which donates and accepts H bond (e.g.: Arg71 of SIRT5) and makes π - π interactions (e.g.: His158 of SIRT5) and the indol-1-one that widely engages in π - π interactions (e.g.: Tyr255 of SIRT5) (Fig. 5a-c).

Cinacalcet is an allosteric activator of the calcium-sensing receptor and used for the treatment of hyperthyroidism and hypercalcemia [35,36]. The compound has no SIRT-related record but it obtained the 7th and 4th best consensus score for SIRT1 and 2, respectively. Cinacalcet's binding to SIRTs was supported by the π - π stacking via its two aromatic rings with for example His 58 and Tyr255 of SIRT5, as well as strong electrostatic contacts via the CF₃ group with the active site residues (Fig. 5d-f). For some SIRTs, the secondary amine was observed to form H bond (see Electronic Supplementary Material for details).

Indacaterol is a β adrenoceptor agonist used for the treatment of chronic obstructive pulmonary disease [37]. The molecule, which ranked the third according to the pan-SIRT scores, has not been tested against SIRTs before. Indacaterol obtained the 2nd and 6th best consensus score for SIRT1 and 3, respectively. The two condensed ring systems of indacaterol greatly contributed to its theoretical binding affinity to SIRTs (Fig. 5g-i). While these rings engaged in π -stacking, for example with residues like Phe64, His133 and Trp188 of SIRT6, the hydroxyl and amino groups made H bonds in most cases to further stabilize the binding (e.g.: His133 and Leu186 of SIRT6).

Pharmacophore models for virtual pan-HDAC and pan-SIRT molecules

Pharmacophore models are hypothetical spatial orientations of the common pharmacophores (functional groups considered important for biological activity) for a set of ligands (or a single ligand) that share a biological property (activity, toxicity, etc.), which are widely exploited in rational drug design applications [38,39]. We created a set of possible pharmacophore hypotheses for virtual pan-HDAC and pan-SIRT inhibitor drug molecules using top three scoring molecules of each group and selected the best hypothesis for each group according to PhaseHypoScore and BEDROC score (scores showing how much a hypothesis fits to the query ligands in general) (Table 4).

The selected hypothesis for virtual pan-HDAC inhibitor drugs (hypothesis 1) consists of a closely located H bond acceptor (A) and donor (D) groups, and a distal ring (R). The alignment of belinostat, bexarotene, and cianidanol with hypothesis 1 clearly show that A and D represent the hydroxamic, carboxylic, and phenolic groups interacting with the zinc and its ligands, while R aligns with the aromatic ring of these compounds that stack with the aromatic side chains of active site residues (Fig. 6a-c). The best hypothesis for alosetron, cinacalcet, and indacaterol (hypothesis 2) features two adjacent rings for the condensed ring of these drugs, a vertical third ring regarding the two for a separate aromatic group, and a hydrophobic group (H) close to the third ring representing a hydrophobic substitution to the third ring, namely methyl, trifluoromethyl, and ethyl (Fig. 6d-f). Thus, hypothesis 2 reflects the hydrophobic nature of SIRT catalytic site. Cianidanol and cinacalcet showed best alignment to hypothesis 1 and 2, respectively (see Fitness score in Table 4).

To test the accordance of these hypothesis with the consensus structure-based hVS campaign, we screened the drug molecules against both hypotheses and compared the results with respect to pan-HDAC and pan-SIRT scores from the molecular docking by calculating 10% enrichment factor (Table 4). This metric shows how many of the drug molecules that are among the top 150 pan-HDAC scoring molecules (i.e., top 10% drugs) are listed in the top 150 compounds according to PhaseScreenScore (score that shows how much a screened molecule fits to the pharmacophore hypothesis) for hypothesis 1. The same goes for pan-HDAC scores and hypothesis 2, as well. Surprisingly, 10% enrichment factor was found 20% for both hypotheses, showing that both methods predicted somewhat similar drug molecules as top virtual pan-HDAC and pan-SIRT inhibitors.

Conclusion

1502 FDA approved drugs were screened against a set of classical HDACs and SIRTs with available crystal structures using FRED, Glide, and AutoDock Vina. The drug molecules were ranked according to their average consensus HDAC and SIRT scores to identify the drug molecules that can potentially inhibit as many HDAC or SIRT isoforms, i.e., virtual pan-HDAC and pan-SIRT inhibitors. The consensus approach in this method works two ways: consensus among the used software and among the isoforms. Belinostat, bexarotene, and cianidanol were the best scoring virtual pan-HDAC inhibitors. Bexarotene and cianidanol have not been tested against HDACs, however these compounds have potential against HDACs and could be repurposed for HDAC-related indications. Specifically, bexarotene may show potent *in vitro* activity against HDAC2 and 6; and cianidanol against HDAC4, 7, and 8. Among these molecules, belinostat is already a confirmed pan-HDAC inhibitor used as an anticancer agent, which shows the success of the hVS methodology. On the other hand, other known pan-HDAC inhibitors such as vorinostat were not listed among the top scoring drugs, which could be considered as a weakness. Alosetron, cinacalcet, and indacaterol obtained the best pan-SIRT scores. Although these compounds have no SIRT record, they may be useful in pan-SIRT-related conditions. Alosetron could be a promising inhibitor of SIRT2, cinacalcet of SIRT1 and 2, and indacaterol of SIRT1 and 3. Bexarotene was also listed among the top-ten pan-SIRT scoring drugs, which could be a potent inhibitor of all HDAC classes and repurposed for a unique indication in this regard. Taken together, these drug molecules may find new indications related to pan-HDAC and pan-SIRT inhibition.

Two pharmacophore hypotheses, one for top pan-HDAC (hypothesis 1) and the other for pan-SIRT scoring drug molecules (hypothesis 2), were created. The top three pan-HDAC and pan-SIRT scoring drugs aligned very well with their respective hypothesis. The pharmacophore features in these hypotheses were in compliance with the binding interactions of the drug molecules predicted by docking. When the drug molecules were screened against the pharmacophore hypotheses and the results were compared with the consensus structure-based hVS, rankings of the molecules according to the pharmacophore and molecular docking screens bore similarities, i.e., some of the top scoring molecules in pharmacophore screens were also among the top pan-HDAC and pan-SIRT scoring drugs. Therefore, both ligand- and structure-based hVS methods yielded compatible results.

References

1. Tang J, Yan H, Zhuang S. Histone deacetylases as targets for treatment of multiple diseases. *Clin Sci*. 2013;124:651-662.
2. Chuang DM, Leng Y, Marinova Z, Kim HJ, Chiu CT. Multiple roles of HDAC inhibition in neurodegenerative conditions. *Trends Neurosci*. 2009;32:591-601.
3. Yoon S, Eom GH. HDAC and HDAC Inhibitor: From Cancer to Cardiovascular Diseases. *Chonnam Med J*. 2016;52:1-11.
4. Barton KM, Archin NM, Keedy KS, Espeseth AS, Zhang YL, Gale J, Wagner FF, Holson EB, Margolis DM. Selective HDAC inhibition for the disruption of latent HIV-1 infection. *PLoS One*. 2014;9:e102684.
5. Goracci L, Deschamps N, Randazzo GM, Petit C, Dos Santos Passos C, Carrupt PA, Simoes-Pires C, Nurisso A. A Rational Approach for the Identification of Non-Hydroxamate HDAC6-Selective Inhibitors. *Sci Rep*. 2016;6:29086.

6. Uciechowska U, Schemies J, Neugebauer RC, Huda EM, Schmitt ML, Meier R, Verdin E, Jung M, Sippl W. Thiobarbiturates as sirtuin inhibitors: virtual screening, free-energy calculations, and biological testing. *ChemMedChem*. 2008;3:1965-1976.
7. Liu J, Zhu Y, He Y, Zhu H, Gao Y, Li Z, Zhu J, Sun X, Fang F, Wen H, Li W. Combined pharmacophore modeling, 3D-QSAR and docking studies to identify novel HDAC inhibitors using drug repurposing. *J Biomol Struct Dyn*. 2020;38:533-547.
8. Pushpakom S, Iorio F, Eyers PA, Escott KJ, Hopper S, Wells A, Doig A, Guilliams T, Latimer J, McNamee C, Norris A, Sanseau P, Cavalla D, Pirmohamed M. Drug repurposing: progress, challenges and recommendations. *Nat Rev Drug Discov*. 2019;18:41-58.
9. McKinsey TA. Isoform-selective HDAC inhibitors: closing in on translational medicine for the heart. *J Mol Cell Cardiol*. 2011;51:491-496.
10. Booth L, Roberts JL, Poklepovic A, Kirkwood J, Dent P. HDAC inhibitors enhance the immunotherapy response of melanoma cells. *Oncotarget*. 2017;8:83155-83170.
11. Amengual JE, Clark-Garvey S, Kalac M, Scotto L, Marchi E, Neylon E, Johannet P, Wei Y, Zain J, O'Connor OA. Sirtuin and pan-class I/II deacetylase (DAC) inhibition is synergistic in preclinical models and clinical studies of lymphoma. *Blood*. 2013;122:2104-2113.
12. Park MA, Mitchell C, Zhang G, Yacoub A, Allegood J, Haussinger D, Reinehr R, Larner A, Spiegel S, Fisher PB, Voelkel-Johnson C, Ogretmen B, Grant S, Dent P. Vorinostat and sorafenib increase CD95 activation in gastrointestinal tumor cells through a Ca(2+)-de novo ceramide-PP2A-reactive oxygen species-dependent signaling pathway. *Cancer Res*. 2010;70:6313-6324.
13. de Lera AR, Ganesan A. Epigenetic polypharmacology: from combination therapy to multitargeted drugs. *Clin Epigenetics*. 2016;8:105.
14. Wishart DS, Feunang YD, Guo AC, Lo EJ, Marcu A, Grant JR, Sajed T, Johnson D, Li C, Sayeeda Z, Assempour N, Iynkkaran I, Liu Y, Maciejewski A, Gale N, Wilson A, Chin L, Cummings R, Le D, Pon A, Knox C, Wilson M. DrugBank 5.0: a major update to the DrugBank database for 2018. *Nucleic Acids Res*. 2018;46:D1074-D1082.
15. Shivakumar D, Williams J, Wu Y, Damm W, Shelley J, Sherman W. Prediction of Absolute Solvation Free Energies using Molecular Dynamics Free Energy Perturbation and the OPLS Force Field. *J Chem Theory Comput*. 2010;6:1509-1519.
16. Friesner RA, Banks JL, Murphy RB, Halgren TA, Klicic JJ, Mainz DT, Repasky MP, Knoll EH, Shelley M, Perry JK, Shaw DE, Francis P, Shenkin PS. Glide: a new approach for rapid, accurate docking and scoring. 1. Method and assessment of docking accuracy. *J Med Chem*. 2004;47:1739-1749.
17. Friesner RA, Murphy RB, Repasky MP, Frye LL, Greenwood JR, Halgren TA, Sanschagrin PC, Mainz DT. Extra precision glide: docking and scoring incorporating a model of hydrophobic enclosure for protein-ligand complexes. *J Med Chem*. 2006;49:6177-6196.
18. Halgren TA, Murphy RB, Friesner RA, Beard HS, Frye LL, Pollard WT, Banks JL. Glide: a new approach for rapid, accurate docking and scoring. 2. Enrichment factors in database screening. *J Med Chem*. 2004;47:1750-1759.
19. McGann M. FRED and HYBRID docking performance on standardized datasets. *J Comput Aided Mol Des*. 2012;26:897-906.
20. O'Boyle NM, Banck M, James CA, Morley C, Vandermeersch T, Hutchison GR. Open Babel: An open chemical toolbox. *ChemInform*. 2011;3:33.
21. Berman HM, Westbrook J, Feng Z, Gilliland G, Bhat TN, Weissig H, Shindyalov IN, Bourne PE. The Protein Data Bank. *Nucleic Acids Res*. 2000;28:235-242.

22. Sastry GM, Adzhigirey M, Day T, Annabhimoju R, Sherman W. Protein and ligand preparation: parameters, protocols, and influence on virtual screening enrichments. *J Comput Aided Mol Des.* 2013;27:221-234.
23. Dallakyan S, Olson AJ. Small-molecule library screening by docking with PyRx. *Methods Mol Biol.* 2015;1263:243-250.
24. Dixon SL, Smondyrev AM, Knoll EH, Rao SN, Shaw DE, Friesner RA. PHASE: a new engine for pharmacophore perception, 3D QSAR model development, and 3D database screening: 1. Methodology and preliminary results. *J Comput Aided Mol Des.* 2006;20:647-671.
25. Lee HY, Chang CY, Su CJ, Huang HL, Mehndiratta S, Chao YH, Hsu CM, Kumar S, Sung TY, Huang YZ, Li YH, Yang CR, Liou JP. 2-(Phenylsulfonyl)quinoline N-hydroxyacrylamides as potent anticancer agents inhibiting histone deacetylase. *Eur J Med Chem.* 2016;122:92-101.
26. Jones P, Altamura S, De Francesco R, Gallinari P, Lahm A, Neddermann P, Rowley M, Serafini S, Steinkuhler C. Probing the elusive catalytic activity of vertebrate class IIa histone deacetylases. *Bioorg Med Chem Lett.* 2008;18:1814-1819.
27. Wang H, Yu N, Chen D, Lee KC, Lye PL, Chang JW, Deng W, Ng MC, Lu T, Khoo ML, Poulsen A, Sangthongpitag K, Wu X, Hu C, Goh KC, Wang X, Fang L, Goh KL, Khng HH, Goh SK, Yeo P, Liu X, Bonday Z, Wood JM, Dymock BW, Kantharaj E, Sun ET. Discovery of (2E)-3-{2-butyl-1-[2-(diethylamino)ethyl]-1H-benzimidazol-5-yl}-N-hydroxyacrylamide (SB939), an orally active histone deacetylase inhibitor with a superior preclinical profile. *J Med Chem.* 2011;54:4694-4720.
28. Mehndiratta S, Wang RS, Huang HL, Su CJ, Hsu CM, Wu YW, Pan SL, Liou JP. 4-Indolyl-N-hydroxyphenylacrylamides as potent HDAC class I and IIB inhibitors in vitro and in vivo. *Eur J Med Chem.* 2017;134:13-23.
29. Hai Y, Christianson DW. Histone deacetylase 6 structure and molecular basis of catalysis and inhibition. *Nat Chem Biol.* 2016;12:741-747.
30. Gniadecki R, Assaf C, Bagot M, Dummer R, Duvic M, Knobler R, Ranki A, Schwandt P, Whittaker S. The optimal use of bexarotene in cutaneous T-cell lymphoma. *Br J Dermatol.* 2007;157:433-440.
31. Fung MT, A.; Mybeck, K.; Wu, J. H.; Hornbuckle, K.; Muniz, E. Evaluation of the Characteristics of Safety Withdrawal of Prescription Drugs from Worldwide Pharmaceutical Markets-1960 to 1999. *Drug Inf J.* 2001;35:293-317.
32. Dai H, Sinclair DA, Ellis JL, Steegborn C. Sirtuin activators and inhibitors: Promises, achievements, and challenges. *Pharmacol Ther.* 2018;188:140-154.
33. Wang HL, Liu S, Wu CY, Cheng LN, Wang YX, Chen K, Zhou S, Chen Q, Yu YM, Li GB. Interactions between sirtuins and fluorogenic small-molecule substrates offer insights into inhibitor design. *Rsc Advances.* 2017;7:36214-36222.
34. Camilleri M, Northcutt AR, Kong S, Dukes GE, McSorley D, Mangel AW. Efficacy and safety of alosetron in women with irritable bowel syndrome: a randomised, placebo-controlled trial. *Lancet.* 2000;355:1035-1040.
35. Ballinger AE, Palmer SC, Nistor I, Craig JC, Strippoli GF. Calcimimetics for secondary hyperparathyroidism in chronic kidney disease patients. *Cochrane Database Syst Rev.* 2014;12:CD006254.
36. Asonitis N, Kassi E, Kokkinos M, Giovanopoulos I, Petychaki F, Gogas H. Hypercalcemia of malignancy treated with cinacalcet. *Endocrinol Diabetes Metab Case Rep.* 2017;2017:17-0118.

37. Beeh KM, Derom E, Kanniss F, Cameron R, Higgins M, van As A. Indacaterol, a novel inhaled beta2-agonist, provides sustained 24-h bronchodilation in asthma. *Eur Respir J*. 2007;29:871-878.

38. Zoete V, Daina A, Bovigny C, Michielin O. SwissSimilarity: A Web Tool for Low to Ultra High Throughput Ligand-Based Virtual Screening. *J Chem Inf Model*. 2016;56:1399-1404.

39. Sari S. Molecular Modelling and Computer Aided Drug Design: The Skill Set Every Scientist in Drug Research Needs and Can Easily Get. *Hujpharm*. 2020;40:34-47

Tables

Table 1 HDAC classes and isoforms

Class I	HDAC1-3, 8
Class IIa	HDAC4, 5, 7, 9
Class IIb	HDAC6, 10
Class III	SIRT1-7
Class IV	HDAC11

Table 2 Top 10 pan-HDAC scoring drugs and their consensus scores for each isoform

Compound	HDAC1	HDAC2	HDAC3	HDAC4	HDAC6	HDAC7	HDAC8	pan-HDAC
Belinostat	-7.3	-9.4	-5.9	-8.5	-9.6	-7.7	-9.1	-8.2
Bexarotene	-6.8	-8.1	-6.2	-9.1	-9.6	-8.0	-8.0	-8.0
Cianidanol	-6.6	-7.0	-6.8	-10.5	-8.1	-8.3	-8.3	-7.9
Phenacemide	-7.0	-8.9	-6.2	-8.2	-8.6	-7.7	-7.1	-7.7
Frovatriptan	-7.2	-7.0	-6.3	-8.5	-8.6	-8.0	-8.1	-7.7
Levodopa	-7.0	-7.8	-5.9	-9.0	-8.0	-7.4	-8.0	-7.6
Chlorphenesin	-6.6	-8.3	-5.5	-8.5	-8.6	-7.3	-8.1	-7.6
Masoprocol	-7.5	-7.0	-6.1	-9.7	-7.7	-7.3	-7.7	-7.6
Benzylparaben	-6.8	-7.7	-6.2	-9.0	-7.3	-8.2	-7.5	-7.5
Ensulizole	-6.8	-7.2	-7.5	-8.8	-7.6	-6.3	-8.4	-7.5

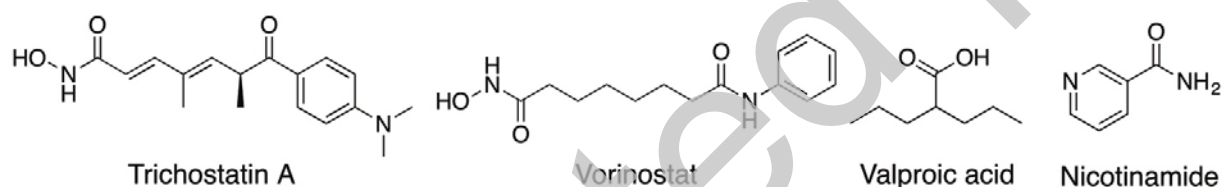
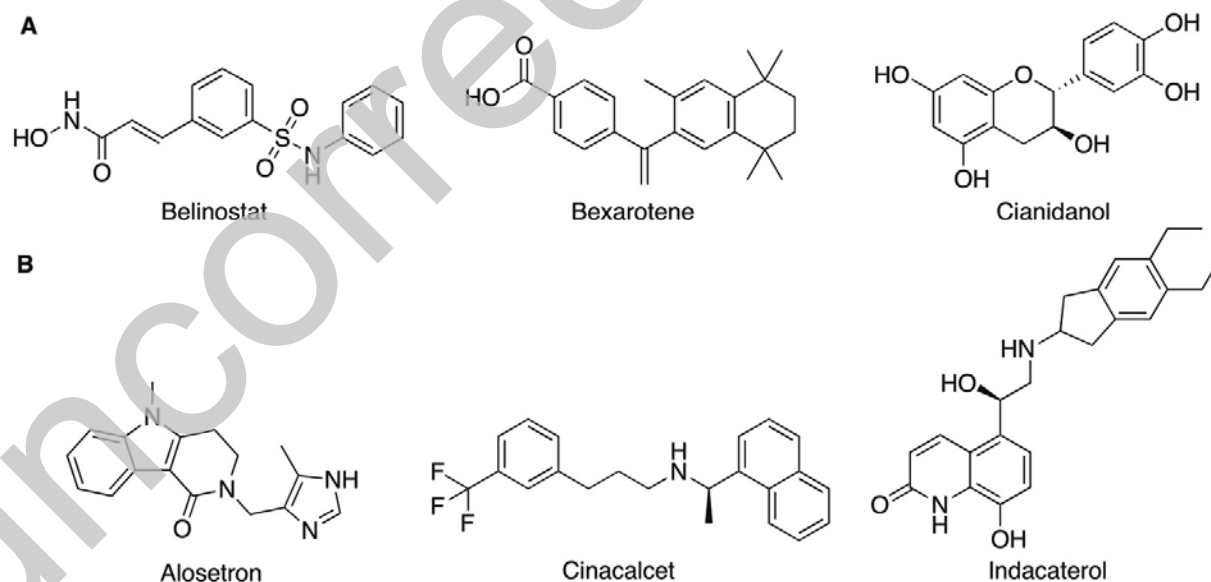
Table 3 Top 10 pan-SIRT scoring drugs and their consensus scores for each isoform

Compound	SIRT1	SIRT2	SIRT3	SIRT5	SIRT6	pan-SIRT
Alosetron	-9.1	-11.4	-7.7	-7.8	-8.5	-8.9
Cinacalcet	-10.1	-11.5	-8.3	-6.7	-7.6	-8.8
Indacaterol	-10.4	-10.1	-8.5	-7.5	-7.6	-8.8
Ziprasidone	-8.8	-12.2	-6.6	-7.8	-8.7	-8.8
Phenprocoumon	-9.6	-10.9	-8.5	-6.7	-8.0	-8.8
Ethinylestradiol	-9.5	-10.4	-7.8	-7.5	-8.6	-8.7
Diffunisal	-9.2	-10.1	-7.5	-8.2	-8.6	-8.7
Bexarotene	-9.7	-11.3	-7.0	-7.2	-8.4	-8.7
Estrone	-9.8	-10.6	-7.4	-7.6	-8.1	-8.7
Tolcapone	-9.3	-10.0	-8.2	-8.0	-7.9	-8.7

Table 4 Pharmacophore hypotheses and their specifications

Hypothesis	Features ¹	PhaseHypoScore	BEDROC Score	Fitness score	10% Enrichment (%)
1	A, D, R	0.95	0.75	belinostat: 2.0 bexarotene: 2.1 cianidanol: 3.0 aloseptron: 1.9	20
2	H, R, R, R	1.20	0.97	cinacalcet: 3.0 indacaterol: 1.8	20

¹ A: H bond acceptor, D: H bond donor, H: hydrophobic, R: ring

**Fig. 1** Known pan-HDAC and pan-SIRT inhibitors**Fig. 2** Catalytic site of HDAC8 (a), HDAC7 (b), HDAC6 (c), and SIRT1. Inhibitors are represented as green stick-ball, zinc as gray sphere, zinc ligands as gray stick, NAD⁺ as teal stick-ball, and protein active sites as solid sphere

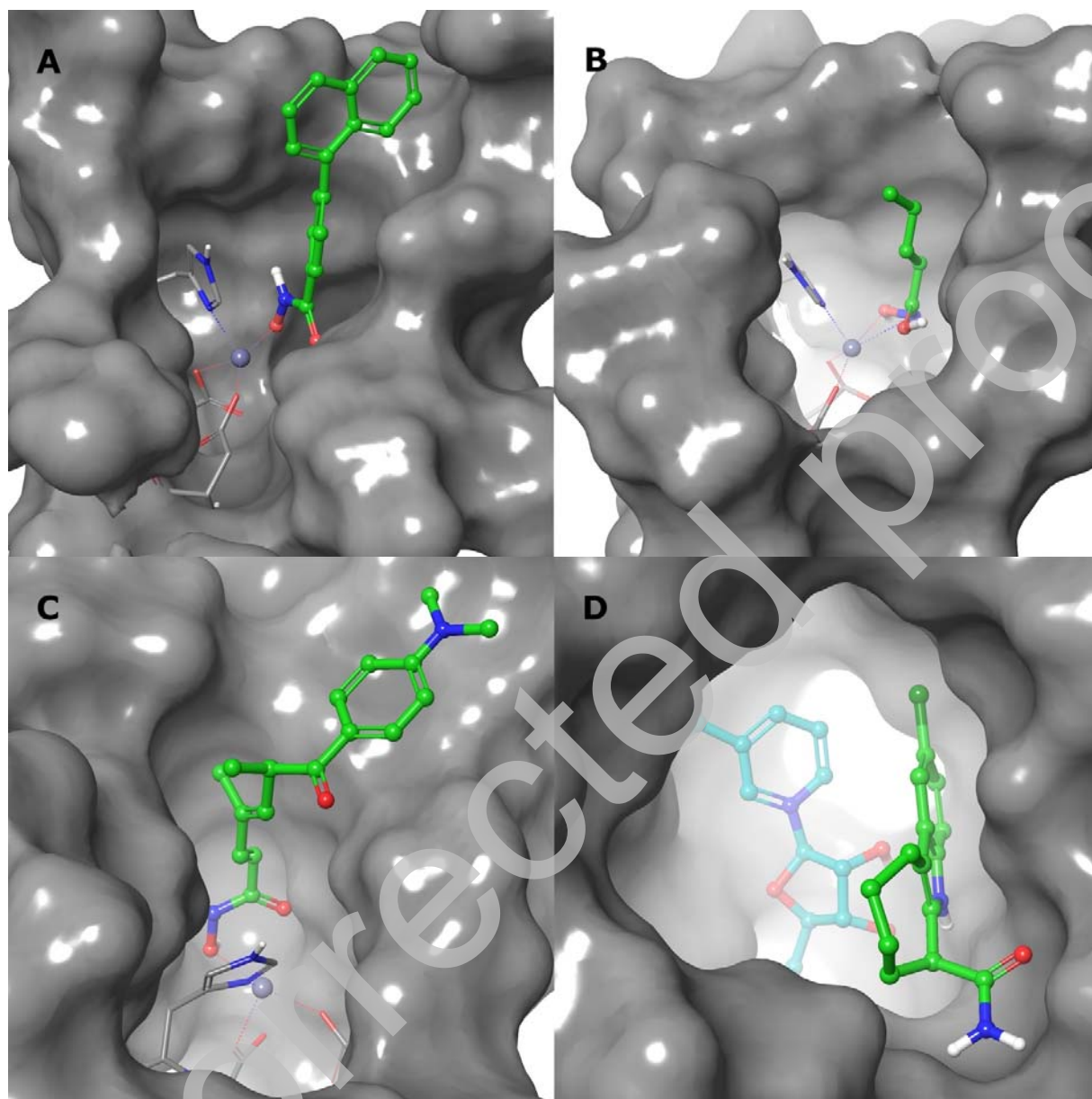


Fig. 3 Top scoring drugs according to pan-HDAC (a) and pan-SIRT (b) scores

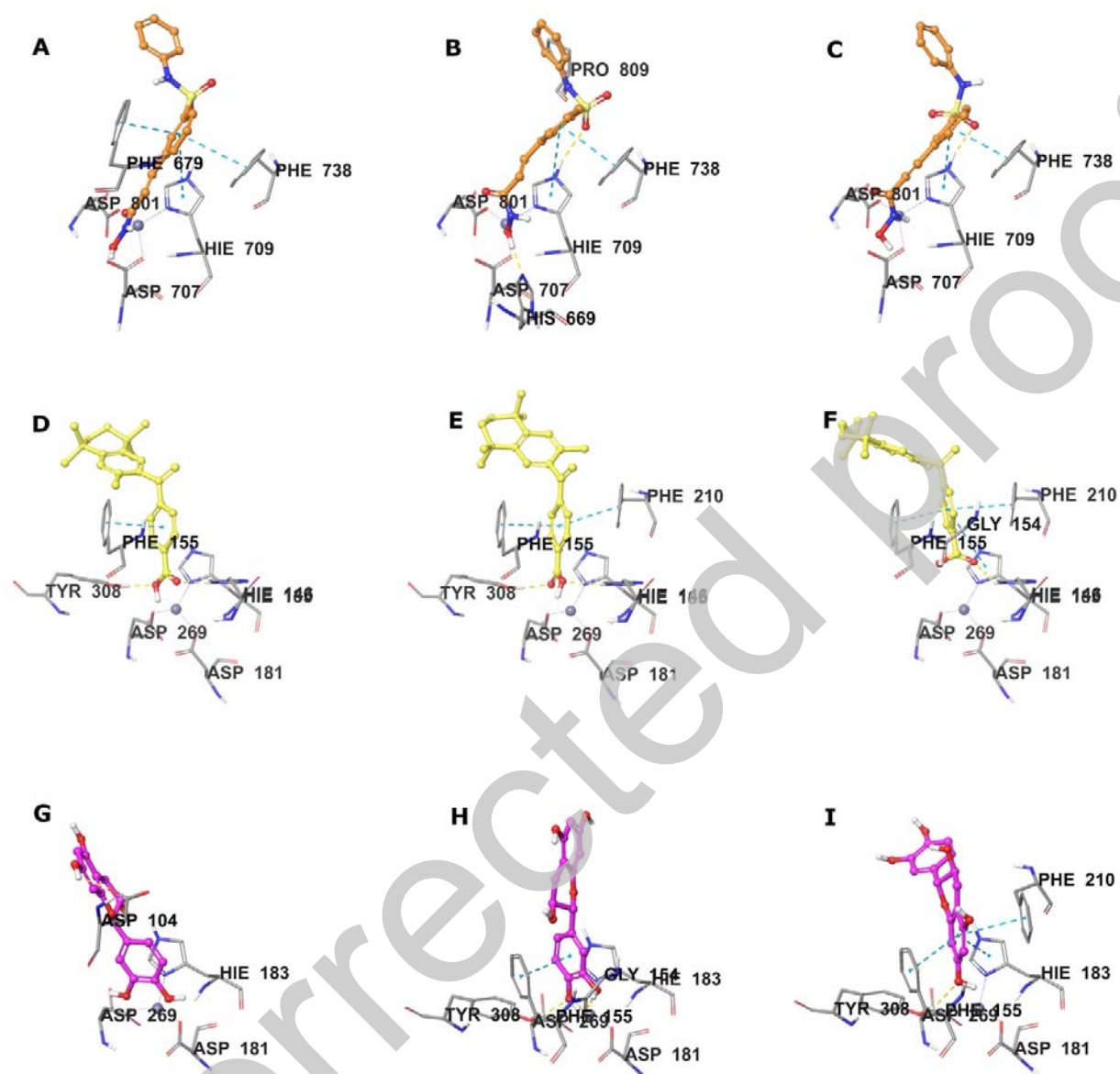


Fig. 4 Binding interactions of belinostat with HDAC7 (a-c), bexarotene with HDAC2 (d-f), and cianidanol with HDAC2 (g-i) predicted by FRED (a, d, g), Glide (b, e, h), and AutoDock Vina (c, f, i), respectively. Drug molecules are represented as color stick-ball, protein residues as gray stick, and interactions as color dash

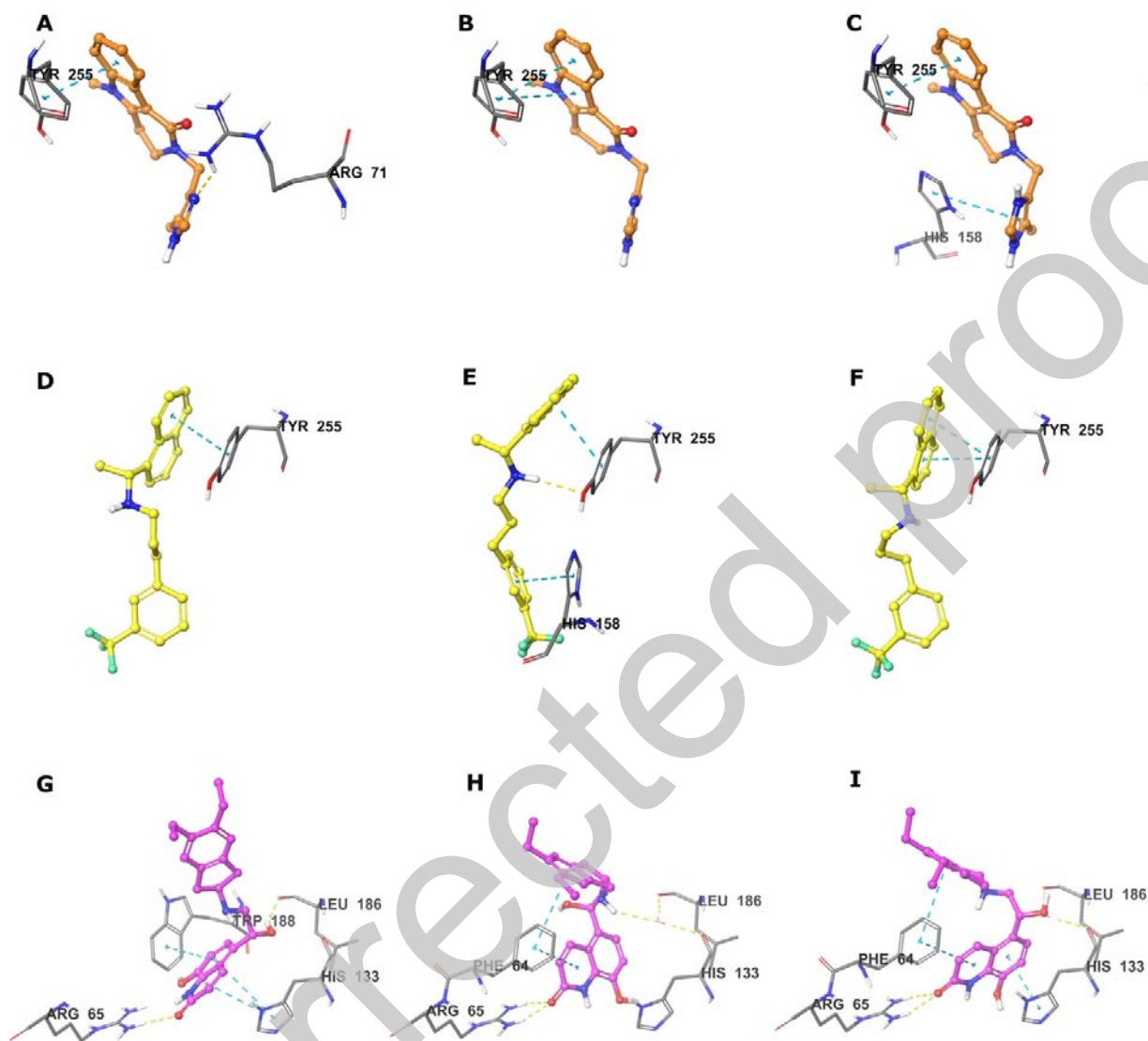


Fig. 5 Binding interactions of alosetron with SIRT5 (a-c), cinacalcet with SIRT5 (d-f), and indacaterol with SIRT6 (g-i) predicted by FRED (a, d, g), Glide (b, e, h), and AutoDock Vina (c, f, i), respectively. Drug molecules are represented as color stick-ball, protein residues as gray stick, and interactions as color dash

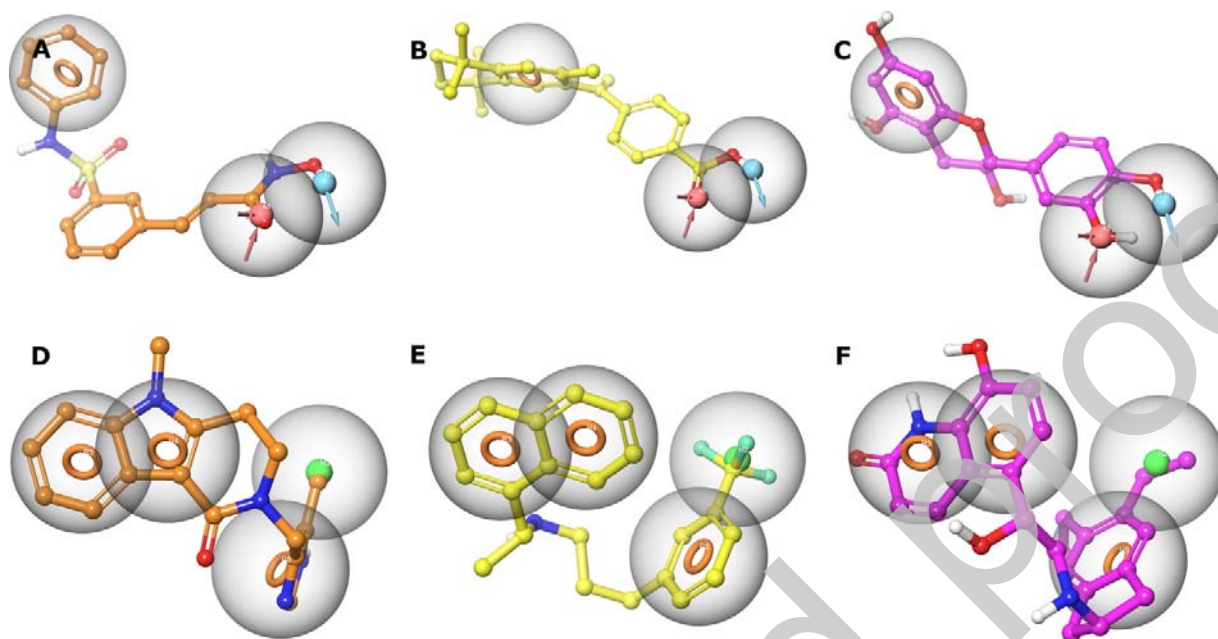


Fig. 6 Hypothesis 1 (a-c) and hypothesis 2 (d-f) aligned with belinostat (a), bexarotene (b), cianidanol (c) alosetron (d), cinacalcet (e), and indacaterol (f). Drug molecules are represented as color stick-ball, pharmacophore features as color ring (ring) and sphere (pink for H bond acceptor, blue for donor, and green for hydrophobic)